Coherent destruction of tunneling and dark Floquet state

2014 New J. Phys. 16 013007

(http://iopscience.iop.org/1367-2630/16/1/013007)

New Journal of Physics
The open access journal at the forefront of physics
Deutsche Physikalische Gesellschaft DPG | IOP Institute of Physics

Coherent destruction of tunneling and dark Floquet state

Xiaobing Luo[1,2], Liping Li[2,3], Li You[2,5] and Biao Wu[4,5,6]

[1] Department of Physics, Jinggangshan University, Ji'an 343009, People's Republic of China
[2] Department of Physics, Tsinghua University, Beijing 100084, People's Republic of China
[3] Information Engineer School, Huanghe Science and Technology College, Zhengzhou 450006, People's Republic of China
[4] International Center for Quantum Materials, Peking University, Beijing 100871, People's Republic of China
[5] Collaborative Innovation Center of Quantum Matter, Beijing, People's Republic of China
E-mail: wubiao@pku.edu.cn

Received 8 September 2013, revised 19 November 2013
Accepted for publication 2 December 2013
Published 9 January 2014
New Journal of Physics **16** (2014) 013007
doi:10.1088/1367-2630/16/1/013007

Abstract

We study a system of three coherently coupled states, where one state is shifted periodically against the other two. We discover that this system possesses a dark Floquet state that has zero quasi-energy and negligible population at the intermediate state. This dark Floquet state manifests itself dynamically in terms of the suppression of inter-state tunneling, a phenomenon known as coherent destruction of tunneling (CDT). Owing to its different origin from the CDT found in a two-state-driven system, we call it dark CDT. At a high-frequency limit for the periodic driving, this Floquet state reduces to the well-known dark state. Our results can be generalized to systems with more states and be verified with easily implemented experiments within the current technologies.

[6] Author to whom any correspondence should be addressed.

1. Introduction

Two-state and three-state models are the simplest quantum systems. Despite their simplicity, they often provide very good approximations to describe realistic physical systems and are capable of revealing a variety of fascinating quantum effects. The understanding of their ubiquitous features is nowadays being exploited for the manipulation and control of the quantum states of small systems involving single atoms, photons or nano-devices [1–3]. Coherent destruction of tunneling (CDT, two-state models) and dark state (three-state models) are two of the elegant prototype examples where a deep understanding gained from the quantum coherent effects in these simple systems is impacting the development of quantum technology in communication and computation.

CDT was discovered in a periodically driving double-well system [4]. It describes a fascinating phenomenon whereby coherent tunneling between two wells (or the Rabi oscillation between two states) is turned off by an externally enforced periodic level shift. Its understanding is related to the dynamical localization [5], which occurs at isolated degenerate points of the quasi-energies [4, 6]. The CDT has thus far generated significant interest, and has been theoretically extended into various forms [7–20]. It has also been observed experimentally in many physical systems, including modulated optical coupler [21], driven double-well potentials for single-particle tunneling [22] and a single electron spin in diamond [23]. More recently, it has also found application in tuning the tunneling parameter of a Bose–Einstein condensate [24, 25].

Dark state is often discussed in terms of a three-state system where two of them are coupled coherently to the intermediate state, as in the model system we study here. When all of the coupling fields are on resonance with their respective coupled pair of states, we can adopt the rotating wave approximation and change it into a suitable interaction picture with all of the coupling coefficients becoming time independent. In this case, there always exists a dark state, whose eigenenergy becomes uniformly zero, and the corresponding eigenvector contains no projection onto the intermediate state. It is called dark as the intermediate state is an excited state capable of emitting photons. This type of dark state is also known as coherent population trapping [26], widely used in efficient population transfer through the stimulated Raman adiabatic passage protocol. It has become the theoretical basis for several well-established implementations of quantum control and rudimentary quantum information processing gates.

In this paper, we report our surprising finding of an intimate relationship between the dark state and the CDT by studying a three-state system. In this system, two states are coherently coupled to an intermediate state and one of the two states shifts periodically against the other two. We find that the CDT also exists in this three-state system, where the dynamical tunneling from one state to the other two is suppressed by the periodic driving over a range of parameters. However, this CDT for the three-state system has its own distinct feature: it is related to a dark Floquet state, which has zero quasi-energy and negligible population at the intermediate state. Quite interestingly, this dark Floquet state reduces to the well-known dark state in a non-driving three-state Λ-system [26] at a high-frequency limit. Therefore, we call this CDT *dark coherent destruction of tunneling* (DCDT). These results can be generalized to the N-state system. We also discuss a feasible experimental scheme where the visualization of the DCDT can be achieved readily.

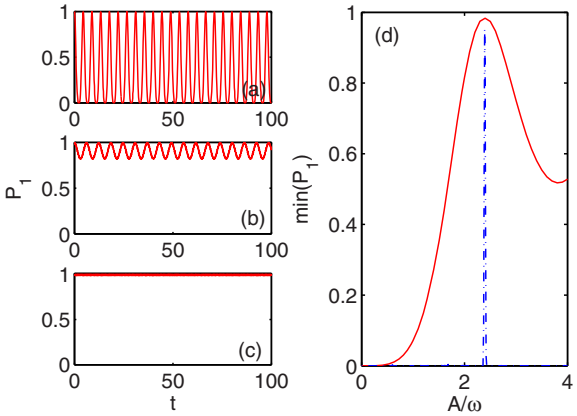

Figure 1. The evolution of the probability at state $|1\rangle$ $P_1 = |c_1|^2$ for the system (1) for various driving conditions: (a) $A/\omega = 0$, (b) $A/\omega = 2.0$ and (c) $A/\omega = 2.4$. (d) The minimum value of P_1 (solid line) as a function of driving parameter A/ω. The two-state results are plotted as a dash-dotted line for comparison. The initial condition is $\{c_1 = 1, c_2 = 0, c_3 = 0\}$. The other parameters are $\omega = 10$, $v = 1$.

2. Three-state system

The driving three-state system is described by the Schrödinger equation ($\hbar = 1$)

$$\begin{aligned} \mathrm{i}\frac{\mathrm{d}c_1}{\mathrm{d}t} &= \frac{A}{2}\sin(\omega t)c_1 + vc_2, \\ \mathrm{i}\frac{\mathrm{d}c_2}{\mathrm{d}t} &= -\frac{A}{2}\sin(\omega t)c_2 + vc_1 + vc_3, \\ \mathrm{i}\frac{\mathrm{d}c_3}{\mathrm{d}t} &= -\frac{A}{2}\sin(\omega t)c_3 + vc_2, \end{aligned} \tag{1}$$

where c_1, c_2 and c_3 are the amplitudes at three states $|1\rangle$, $|2\rangle$ and $|3\rangle$, respectively. v is the coupling constant between the neighboring states. Energy state $|1\rangle$ is shifted periodically against the other two with driving strength A and frequency ω. The normalization condition $\Sigma_{j=1}^{3}|c_j|^2 = 1$ is assumed.

To investigate the tunneling dynamics, we solve the time-dependent Schrödinger equation (1) numerically with the initial state $(1, 0, 0)^{\mathrm{T}}$. The evolution of the probability distribution $P_1 = |c_1|^2$ is presented in figure 1 for three typical driving conditions. For $A/\omega = 0$ (figure 1(a)), we see that P_1 oscillates between zero and one, demonstrating no suppression of tunneling. For $A/\omega = 2.0$ (figure 1(b)), the oscillations of P_1 are seen limited between 0.8 and 1, showing the suppression of tunneling. At $A/\omega = 2.4$ (figure 1(c)), P_1 remains near unity, signaling a complete suppression of tunneling between the energy states. This is the quantum phenomenon well known as CDT [4].

We emphasize that what we find here is not a simple re-discovery of the CDT in a three-state system. The CDT in this three-state model has its own distinct feature: the results shown in figures 1(b) and (c) indicate that the suppression of tunneling occurs over a wide range of system parameters. This is in stark contrast to the CDT in a two-state system [4], which occurs only at isolated points of the parameters. The widening of the suppression regime found in the driving three-state system is more clearly demonstrated in figure 1(d), where the minimum

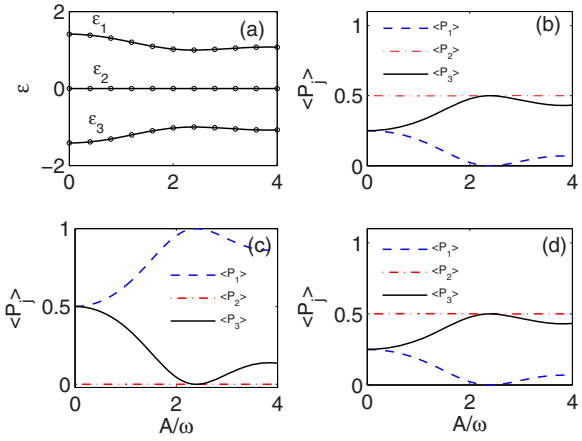

Figure 2. (a) Quasi-energies versus A/ω. Solid lines are for numerical results obtained from the original model (1) and the circles are for the approximation results given by the effective model (3). The time-averaged populations for the Floquet state in the quasi-energy level (b) ε_1, (c) ε_2 and (d) ε_3. The other parameters are $v = 1$, $\omega = 10$.

value of P_1 is used to measure the suppression of the tunneling. When $\min(P_1)$ is not zero, the tunneling is suppressed as the population is not allowed to be fully transferred from state $|1\rangle$ to the other two states. It is clear from figure 1(d) that the suppression occurs as long as $A/\omega \neq 0$. For comparison, the results for the standard driven two-state system are plotted as dash-dotted line in figure 1(d), where the extremely narrow peak width indicates that the CDT occurs only at isolated points of the parameters.

There exists a fundamental reason that the CDT occurs at the isolated system parameters in a two-state model: the CDT in the two-state model is related to the degeneracy of the quasi-energy levels [4] and the degeneracy usually happens only at the isolated points. Therefore, the significant widening of the suppression parameter range that we see in figure 1 indicates that the CDT found here should have a different origin. To find this origin, we turn to the Floquet theory for a periodically driving system. Similar to the Bloch states for systems with spatially periodic potentials, the modulated system (1) has Floquet states, $(c_1, c_2, c_3)^{\mathrm{T}} = (\tilde{c}_1, \tilde{c}_2, \tilde{c}_3)^{\mathrm{T}} \exp(-\mathrm{i}\varepsilon t)$, where ε is the quasi-energy and the amplitudes $(\tilde{c}_1, \tilde{c}_2, \tilde{c}_3)^{\mathrm{T}}$ are periodic of the modulation period $T = 2\pi/\omega$.

Our numerical results of the quasi-energies and the Floquet states for the modulated system (1) are plotted in figure 2. There are three Floquet states with quasi-energies ε_1, ε_2 and ε_3. We immediately notice from figure 2(a) that the quasi-energy ε_2 for the second Floquet state is always *zero* for all of the values of A/ω. We call this state *dark Floquet state* in analogy to the well-known dark state. This dark Floquet state stands out not only for its zero quasi-energy but also for its unique population distribution among the energy states. We display the time-averaged population probability $\langle P_j \rangle = (\int_0^{\mathrm{T}} \mathrm{d}t |c_j|^2)/T$ for a given Floquet state $(c_1, c_2, c_3)^{\mathrm{T}}$ in figures 2(b)–(d). Note that the time-averaged populations are almost independent of the frequency in the high-frequency regime. The Floquet state with $\langle P_j \rangle > 0.5$ is generally regarded as a state localized at the jth energy state. As seen in figure 2(c), the dark Floquet state has almost zero population at energy state $|2\rangle$ while the population $\langle P_1 \rangle > 0.5$ at $|1\rangle$. In other words, the dark Floquet state is localized at $|1\rangle$. The other two Floquet states have identical population distribution. Since all of their populations $\langle P_j \rangle \leqslant 0.5$, these two Floquet states are *not* localized.

We note that a Floquet state with zero quasi-energy was also found in [19]. However, it is not related to the CDT discovered in the same system and its relation to the dark state is not discussed.

It is not difficult to see the suppression of the tunneling seen in figure 1 is linked to the existence of the dark Floquet state. We expand the initial state in terms of the Floquet states

$$(1, 0, 0)^{\mathrm{T}} = b_1|\varepsilon_1\rangle + b_2|\varepsilon_2\rangle + b_3|\varepsilon_3\rangle. \tag{2}$$

During the dynamical evolution, the expansion coefficient b_i evolves as $b_i \exp(-\mathrm{i}\varepsilon_i t)$. Hence, the $|b_i|$'s are time independent. We look at the case $A/\omega = 2.4$, where $|\varepsilon_2\rangle$ has population one at state $|1\rangle$ while the other two states have zero population at $|1\rangle$. In this case, we have $|b_2| = 1$ and $b_1 = b_3 = 0$, which corresponds to a complete suppression of the tunneling from $|1\rangle$ to $|2\rangle$ and $|3\rangle$. For the other values of A/ω, similar arguments can be made. This shows that the CDT observed in figure 1 has a different origin: it is the consequence of the dark Floquet states. Therefore, we call it *dark coherent destruction of tunneling* (DCDT).

Interestingly, this dark Floquet state can be reduced to the well-known dark state in a non-driven three-state Λ-system at a high-frequency limit. By introducing the transformation $c_m = a_m \exp[\pm \mathrm{i}A\cos(\omega t)/(2\omega)]$ (+ for $m = 1$ and $-$ for $m = 2, 3$) and averaging out the high-frequency terms, one can obtain a non-driven three-state system

$$\begin{aligned}
\mathrm{i}\frac{\mathrm{d}a_1}{\mathrm{d}t} &= vJ_0(A/\omega)a_2,\\
\mathrm{i}\frac{\mathrm{d}a_2}{\mathrm{d}t} &= vJ_0(A/\omega)a_1 + va_3,\\
\mathrm{i}\frac{\mathrm{d}a_3}{\mathrm{d}t} &= va_2,
\end{aligned} \tag{3}$$

where $J_0(A/\omega)$ is the zeroth-order Bessel function. The famous dark state (also known as coherent trapped state) for equation (3) is given by $(a_1, a_2, a_3)^{\mathrm{T}} = \frac{1}{\sqrt{\mathcal{M}}}(-v, 0, vJ_0(A/\omega))^{\mathrm{T}}$, where $\mathcal{M} = v^2 + [vJ_0(A/\omega)]^2$. This dark state corresponds to the dark Floquet state. Similarly, this dark state is always localized at state $|1\rangle$ as $v^2 > [vJ_0(A/\omega)]^2$ and has zero population at state $|2\rangle$. This state is completely localized at state $|1\rangle$ when $J_0(A/\omega) = 0$. We have computed the eigenvalues of model (3) and compared them (circles) with the quasi-energies (black solid lines) in figure 2(a). The agreement is almost perfect.

3. Generalization to the *N*-state system

Our analysis above is given for a three-state system and the original CDT was found in a two-state system. These results can be generalized to an N-state system, where one state is shifted periodically against all of the other states. The equations of motion are

$$\begin{aligned}
\mathrm{i}\frac{\mathrm{d}c_j}{\mathrm{d}t} &= v(c_{j-1} + c_{j+1}) + F_j(t)c_j,\\
F_1(t) &= \frac{A}{2}\sin(\omega t),\quad F_{j\neq 1}(t) = -\frac{A}{2}\sin(\omega t),
\end{aligned} \tag{4}$$

where $c_{j\leqslant 0} = c_{j>N} = 0$.

The quantum dynamics of the driven N-state systems is investigated by direct integration of the time-dependent Schrödinger equation (4) with the state initially prepared on the state $|1\rangle$.

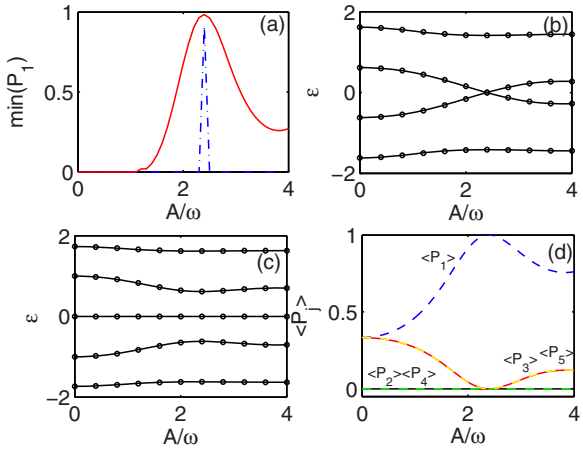

Figure 3. (a) The minimum value of P_1 as a function of A/ω for $N = 4$ (dash dotted line) and $N = 5$ (solid line). The initial conditions are $c_1(0) = 1, c_j(0) = 0 (j \neq 1)$. Quasi-energies versus A/ω for (b) $N = 4$ and (c) $N = 5$. The solid lines are for the numerical results obtained from the model (4) and the circles are for the approximation results given by the effective model (5). (d) The time-averaged probability distribution of the Floquet state corresponding to $\varepsilon = 0$ in figure 3(c). The other parameters are $v = 1, \omega = 10$.

The CDT is found to exist. The minimum value of $P_1 = |c_1|^2$ as a function of A/ω is presented in figure 3(a) for $N = 4$ and 5. When $N = 4$, the CDT occurs at an isolated point of parameters (dash dotted line in figure 3(a)), where two of the four quasi-energy levels become degenerate (figure 3(b)). This is exactly the same as in the two-state system. When $N = 5$, the parameter range where CDT occurs is extended substantially (solid line in figure 3(a)) as in the three-state model. Furthermore, this five-state system also has a dark Floquet state: as seen in figure 3(c), one of the quasi-energies always equals to zero. This dark Floquet state has negligible population at all of the even jth states (figure 3(d)).

These numerical results with $N = 4, 5$, together with the known results for $N = 2, 3$, clearly suggest that (i) the dark Floquet state and the associated DCDT exist in all of the odd-N-state systems; and (ii) the original CDT, which occurs at the isolated parameter points, exists in all of the even-N-state systems. This general conclusion can be proved analytically at a high-frequency limit.

Following the procedure used in the three-state system, we introduce the transformation $c_1 = a_1 \exp[-\mathrm{i}\int A\sin(\omega t)/2\,\mathrm{d}t]$, $c_{j\neq 1} = a_j \exp[\mathrm{i}\int A\sin(\omega t)/2\,\mathrm{d}t]$, where $a_j(z)$ are slowly varying functions. By using the expansion $\exp[\pm \mathrm{i}A\cos(\omega t)/\omega] = \sum_k (\pm\mathrm{i})^k J_k(A/\omega)\exp(\pm \mathrm{i}k\omega t)$ in terms of the Bessel functions and neglecting all of the orders except $k = 0$ for a high-frequency limit, we can reduce the coupled equations (4) to a non-driven model

$$\mathrm{i}\frac{\mathrm{d}\mathbf{a}}{\mathrm{d}t} = \bar{H}\mathbf{a}, \tag{5}$$

where $\mathbf{a} = (a_1, a_2, \ldots, a_N)^{\mathrm{T}}$. The matrix $\bar{H}$ is tridiagonal with non-zero elements $\bar{H}_{12} = \bar{H}_{21} = v_{\mathrm{eff}} = vJ_0(A/\omega)$, $\bar{H}_{n,n+1} = \bar{H}_{n+1,n} = v$ for $n = 2, \ldots, N-1$. The effective coupling constant v_{eff} between state $|1\rangle$ and state $|2\rangle$ is tunable with the driving parameters.

The eigenvalues and the eigenvectors of the tridiagonal $N \times N$ matrix $\bar{H}$ enjoy some very interesting properties, whose rigorous proofs can be found in the appendix.

(a) *When N is even, for any non-zero v_{eff} and v, all of the eigenvalues of the matrix $\bar{H}$ are non-zero while two of the eigenvalues are zero for $v_{\text{eff}} = 0$.*

Remark 1. *This means that when N is even, two quasi-energy levels of the driven model (4) are degenerate at the isolated points where $v_{\text{eff}} = vJ_0(A/\omega) = 0$. The CDT occurs at these isolated points.*

(b) *When N is odd, one and only one eigenvalue of $\bar{H}$ always equals to zero and, for the corresponding eigenvector $(w_1, w_2, \ldots, w_N)^{\mathrm{T}}$ of $\bar{H}$, the inequality $|w_1|^2 > 0.5$ holds for a finite range of parameters; for any other eigenvector $(w_1, w_2, \ldots, w_N)^{\mathrm{T}}$ of $\bar{H}$, one has $|w_j|^2 \leqslant 0.5$.*

Remark 2. *When N is odd, the system always has one and only one dark Floquet state, which is localized over a finite range of parameters. Correspondingly, the DCDT occurs over a finite range of parameters.*

4. Experimental observation

By mapping the temporal evolution of the quantum systems into the spatial propagations of the light waves, the engineered waveguides have provided an ideal platform to investigate a wide variety of coherent quantum effects [27, 28]. The phenomenon of the DCDT can also be observed with this kind of waveguide system. The discrete model (4) can be simulated by the light propagation in an array of N waveguides placed closely and with equal spacing.

In optics, the electric field $\phi(x, z)$ of light obeys the wave equation [29, 30]

$$\mathrm{i}\frac{\partial \phi}{\partial z} = -\frac{1}{2}\frac{\partial^2 \phi}{\partial x^2} - pR(x, z)\phi. \tag{6}$$

Here x and z are the normalized transverse and longitudinal coordinates, and p describes the refractive index contrast of the individual waveguide. Periodic driving is realized by the harmonic modulation of the refractive index of the waveguides along the propagation direction [29, 30]. For our system, the periodic modulation of the first waveguide has a phase difference of π against the modulations for all of the other $N-1$ waveguides. The corresponding refractive index distribution of this kind of waveguide system is given by

$$R(x, z) = \sum_{j=-(N-2)}^{1} \left[1 + f_j(z)\right] \exp\left[-\left(\frac{x - jw_{\mathrm{s}}}{w_x}\right)^6\right], \tag{7}$$

$$f_1(z) = \mu \sin(\omega z), \quad f_j(z) = -\mu \sin(\omega z)\ (j \neq 1)$$

with the waveguide spacing w_{s}, the channel width w_x, the longitudinal modulation amplitude μ and the modulation frequency ω. Therein the super-Gaussian function $\exp(-x^6/w_x^6)$ describes the profile of the individual waveguides with widths w_x.

To investigate the dynamics of the light tunneling, we simulate the modulated waveguides array ($N = 2$, as in figure 4(a); and $N = 3$, as in figure 4(b)) by integrating the continuous wave equation (6). In our numerical simulation, the initial states are chosen as the lowest Wannier modes for the isolated individual waveguides, and the dimensionless parameters are

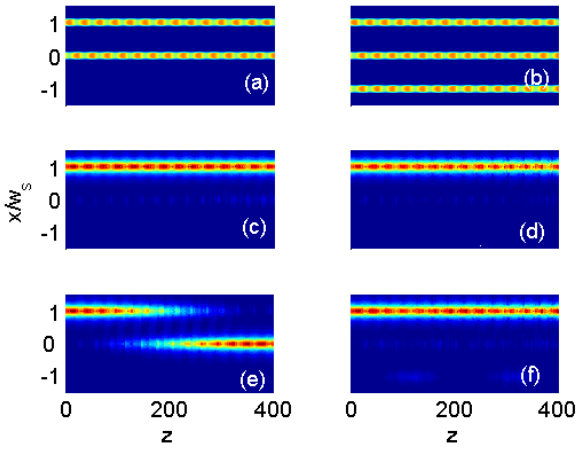

Figure 4. The refractive index distribution $R(x, z)$ of a waveguide array for (a) $N = 2$ and (b) $N = 3$. Propagation dynamics $|\phi(x, z)|^2$ in a two-channel waveguide (a) at (c) $\mu = 0.2$; (e) $\mu = 0.18$, and a three-channel waveguide (b) at (d) $\mu = 0.2$; (f) $\mu = 0.18$. The other parameters are seen in the text. In all of the cases, the top waveguide is excited at $z = 0$.

set as $w_x = 0.3$, $w_s = 3.2$, $p = 2.78$ and $\omega = 3.45 \times (2\pi/100)$. As in the current experimental setup [29, 30], w_x and w_s are in units of $10\,\mu$m, and $p = 2.78$ corresponds to a real refractive index of 3.1×10^{-4}.

The dynamics of the light tunneling is visualized in figure 4. A perfect tunneling inhibition is illustrated in figures 4(c) and (d) at $\mu = 0.2$ which corresponds to the degeneracy point of the quasi-energy levels in the two-state system. When the modulation amplitude is slightly detuned from $\mu = 0.2$ to 0.18, no suppression of the tunneling occurs in the two-channel waveguide (see figure 4(e)), while the strong suppression of tunneling is still observed in the three-channel waveguide (see figure 4(f)). Our numerical simulations of the continuous wave equation (6) confirm the widening of the suppression regime predicted by the driving three-state model (1). Moreover, we have simulated the other waveguide systems with more than three waveguides by directly integrating the continuous wave equation (6) (not shown here). These numerical results verify firmly the existence of the DCDT in the odd-N-state systems.

The discrete model (1) also describes the dynamics of a quantum particle in a triple-well system where one well is periodically driven with respect to the others. The driving field applied to our system is different from those extensively studied in the literature where the CDT is caused by the level degeneracy rather than the dark Floquet state. The advantage of our driving is that it can be used to manipulate the population distribution of the dark Floquet state and thus produce a novel phenomenon of the DCDT. Another possibility to realize the discrete model (1) is a three-level Λ-system. Let us consider three energy levels $|1\rangle$, $|2\rangle$ and $|3\rangle$. Two metastable states $|1\rangle$ and $|3\rangle$ are coherently coupled to the intermediate state $|2\rangle$ via a pump laser with frequency ω_p and a dump laser with frequency ω_d. We fix the pump laser frequency ω_p and chirp the dump laser frequency as $\omega_d = \omega_d' + A\sin(\omega t)/\hbar$ with ω_d' constant. By setting one-photon detuning $E_2 - E_1 - \hbar\omega_p = 0$ and two-photon detuning $E_3 - E_1 - (\hbar\omega_p - \hbar\omega_d) = A\sin(\omega t)$, the effective Hamiltonian in the rotating wave approximation can be reduced to the discrete model (1) in which the coupling strength between the states is determined by the pulsed Rabi frequencies.

5. Conclusion

In summary, we find that the CDT also happens in a three-state quantum system, where one energy state is shifted periodically against the other two states. We call this type of CDT dark coherent destruction of tunneling (DCDT) as it is related to the existence of a dark Floquet state in this three-state system. The dark Floquet state has zero quasi-energy and negligible population at the intermediate state. It reduces to the well-known dark state of a non-driven three-state system at a high-frequency limit. These results can be generalized to a periodically driven N-state system. We have also pointed out that the observation of the DCDT is well within the capacity of the current experiments.

Acknowledgments

This work is funded by the NSF of China (10965001, 11165009), the NSF of Jiangxi Province (2010GQW0033), NCET-13-0836, the Jiangxi Young Scientists Training Plan (20112BCB23024), Scientific and Technological Research Fund of Jiangxi Provincial Education Department (numbers GJJ13542, GJJ12483), the financial support provided by the Key Subject of Atomic and Molecular Physics in Jiangxi Province and Zhengzhou MBOST (20120409). BW was supported by the NBRP of China (2012CB921300,2013CB921900), the NSF of China (11274024), the RFDP of China (20110001110091). LY was supported by the NSF of China (11004116) and by MOST 2013CB922000 of the National Key Basic Research Program of China.

Appendix

The $N \times N$ tridiagonal matrix $\bar{H}$ has the following non-zero matrix elements: $\bar{H}_{12} = \bar{H}_{21} = v_{\rm eff}$, $\bar{H}_{n,n+1} = \bar{H}_{n+1,n} = v$ for $n = 2, \ldots, N-1$. $v_{\rm eff}$ is tunable and $v \neq 0$ is fixed. The eigenvalues and the eigenvectors of $\bar{H}$ have the following properties.

Property 1. *When N is odd, one and only one eigenvalue of $\bar{H}$ always equals to zero.*

Proof. Let $\lambda_1, \lambda_2, \ldots, \lambda_N$ be all of the eigenvalues of the matrix $\bar{H}$, then $D_N = \det(\bar{H}) = \lambda_1\lambda_2\cdots\lambda_N$. It is easy to verify that $D_2 = -v_{\rm eff}^2$, $D_1 = D_3 = 0$ and the relation $D_N = -v^2 D_{N-2} (N \geqslant 3)$. Therefore, one has $D_{2k-1} = 0$ and $D_{2k} = (-1)^k v^{2k-2} v_{\rm eff}^2$ $(k = 1, 2, 3, \ldots)$. When N is odd, $D_N = \lambda_1\lambda_2\cdots\lambda_N = 0$, which means that at least one eigenvalue equals to zero regardless of the values of $v_{\rm eff}$ and v. For the zero eigenvalue, the eigenequation is $\bar{H}\mathbf{w} = 0$, where $\mathbf{w} = (w_1, w_2, \ldots, w_N)^{\rm T}$. When expanded, the equation is turned into the following equations: $v_{\rm eff} w_2 = 0$, $v_{\rm eff} w_1 + v w_3 = 0$, $v w_{j-1} + v w_{j+1} = 0$ $(j = 3, 4, \ldots, N-1)$, $v w_{N-1} = 0$. There is only one non-trivial solution. For $v_{\rm eff} \neq 0$, it is given by

$$\mathbf{w} = \frac{1}{\sqrt{\mathcal{M}}}(w_1^0, w_2^0, \ldots, w_N^0)^{\rm T} \tag{A.1}$$

with $w_1^0 = (-1)^{(N-1)/2} v / v_{\rm eff}$, $w_{2k}^0 = 0$, and $w_{2k+1}^0 = (-1)^{(N-2k-1)/2}$ where $k = 1, 2, \ldots, (N-1)/2$ and $\mathcal{M} = \sum_{j=1}^{N} |w_j^0|^2$ is the normalization factor. For $v_{\rm eff} = 0$, the solution is $\mathbf{w} = (1, 0, \ldots, 0)^{\rm T}$. This shows that matrix $\bar{H}$ has one and only one eigenvalue equal to zero. □

Property 2. *When N is even, for any non-zero $v_{\rm eff}$, all of the eigenvalues of the matrix $\bar{H}$ are non-zero while two of the eigenvalues are zero for $v_{\rm eff} = 0$.*

Proof. If $v_{\rm eff} \neq 0$, when N is even, then $D_N = (-1)^{N/2} v^{N-2} v_{\rm eff}^2 = \lambda_1 \lambda_2 \cdots \lambda_N \neq 0$. Thus, all of the eigenvalues of the matrix $\bar{H}$ are non-zero. When $v_{\rm eff} = 0$, it is obvious that $D_N = \lambda_1 \lambda_2 \cdots \lambda_N = 0$. There are zero eigenvalues. With $v_{\rm eff} = 0$, the tridiagonal matrix of $\bar{H}$ is divided into two uncoupled subspaces, i.e. $\bar{H} = 0 \oplus F$, where F is a tridiagonal matrix with non-zero elements $F_{n,n+1} = F_{n+1,n} = v$. It is clear that F possesses property 1 and has only one zero eigenvalue. $\bar{H}$ thus has two zero eigenvalues. □

Property 3. *If λ is an eigenvalue of $\bar{H}$ with eigenvector $(w_1, w_2, \ldots, w_N)^{\rm T}$, then $-\lambda$ is an eigenvalue of $\bar{H}$ with the corresponding eigenvector $(w'_1, w'_2, \ldots, w'_N)^{\rm T}$ where $w'_j = (-1)^j w_j$.*

Proof. The eigenvalue equation $\bar{H}\mathbf{w} = \lambda \mathbf{w}$ can be written in the form $\Sigma_{j=1}^{N} \bar{H}_{ij} w_j = \lambda w_i$, where $\bar{H}_{ij} = 0$ when $|i - j| = 0$ and $|i - j| \geqslant 2$. Multiplying by $(-1)^{i-1}\lambda$, we obtain $\Sigma_{j=1}^{N} \bar{H}_{ij} (-1)^j w_j = -\lambda (-1)^i w_i$ and have the proof. □

Property 4. *When N is odd, for the eigenvector $(w_1, w_2, \ldots, w_N)^{\rm T}$ of $\bar{H}$ belonging to $\lambda = 0$, the inequality $|w_1|^2 > 1/2$ holds for a finite range of parameters; For an eigenvector $(w_1, w_2, \ldots, w_N)^{\rm T}$ of $\bar{H}$ belonging to $\lambda \neq 0$, one has that $|w_j|^2 \leqslant 1/2$, whether N is odd or even.*

Proof. According to equation (A.1), it is clear that the inequality $|w_1|^2 > 0.5$ is valid only when $(v/v_{\rm eff})^2 > (N-1)/2$. When $\lambda \neq 0$, the two eigenvalues λ and $-\lambda$ are distinct and the corresponding eigenvectors are orthogonal to each other. With property 3, one has $\Sigma_{k=1}^{(N+1)/2} |w_{2k-1}|^2 = \Sigma_{k=1}^{(N-1)/2} |w_{2k}|^2$ when N is odd; $\Sigma_{k=1}^{N/2} |w_{2k-1}|^2 = \Sigma_{k=1}^{N/2} |w_{2k}|^2$ when N is even. With the normalization condition $\Sigma_{j=1}^{N} |w_j|^2 = 1$, we immediately obtain that $|w_j|^2 \leqslant 0.5$. □

References

[1] Brif C, Chakrabarti R and Rabitz H 2010 *New J. Phys.* **12** 075008
[2] Salger T, Kling S, King T, Geckeler C, Molina L M and Weitz M 2009 *Science* **326** 1241
[3] Grifoni M and Hänggi P 1998 *Phys. Rep.* **304** 229
[4] Grossmann F, Dittrich T, Jung P and Hanggi P 1991 *Phys. Rev. Lett.* **67** 516
Grossmann F, Dittrich T, Jung P and Hanggi P 1991 *Z. Phys.* B **84** 315
[5] Dunlap D H and Kenkre V M 1986 *Phys. Rev.* B **34** 3625
[6] Holthaus M 1992 *Phys. Rev. Lett.* **69** 351
Holthaus M and Hone D 1993 *Phys. Rev.* B **47** 6499
[7] Creffield C E 2007 *Phys. Rev. Lett.* **99** 110501
[8] Gong J, Poletti D and Hanggi P 2007 *Phys. Rev.* A **75** 033602
[9] Luo X, Huang J and Lee C 2011 *Phys. Rev.* A **84** 053847
[10] Longhi S 2005 *Phys. Rev.* A **71** 065801
Longhi S and Della Valle G 2012 *Phys. Rev.* A **86** 042104
[11] Villas-Bôas J M, Ulloa S E and Studart N 2004 *Phys. Rev.* B **70** 041302
[12] Stockburger J T 1999 *Phys. Rev.* E **59** R4709

[13] Luo X, Xie Q and Wu B 2007 *Phys. Rev.* A **76** 051802
[14] Gong J, Morales-Molina L and Hänggi P 2009 *Phys. Rev. Lett.* **103** 133002
[15] Longhi S 2011 *Phys. Rev.* A **83** 034102
Longhi S 2012 *Phys. Rev.* A **86** 044102
[16] Creffield C E and Monteiro T S 2006 *Phys. Rev. Lett.* **96** 210403
Creffield C E 2007 *Phys. Rev.* A **75** 031607
[17] Eckardt A, Weiss C and Holthaus M 2005 *Phys. Rev. Lett.* **95** 260404
Eckardt A and Holthaus M 2008 *Phys. Rev. Lett.* **101** 245302
[18] Hai W, Hai K and Chen Q 2013 *Phys. Rev.* A **87** 023403
[19] Lu G, Hai W and Xie Q 2011 *Phys. Rev.* A **83** 013407
[20] Kayanuma Y and Saito K 2008 *Phys. Rev.* A **77** 010101
[21] Della Valle G, Ornigotti M, Cianci E, Foglietti V, Laporta P and Longhi S 2007 *Phys. Rev. Lett.* **98** 263601
[22] Kierig E, Schnorrberger U, Schietinger A, Tomkovic J and Oberthaler M K 2008 *Phys. Rev. Lett.* **100** 190405
[23] Zhou J, Huang P, Zhang Q, Wang Z, Tan T, Xu X, Shi F, Rong X, Ashhab S and Du J 2013 arXiv:1305.0157
[24] Lignier H, Sias C, Ciampini D, Singh Y, Zenesini A, Morsch O and Arimondo E 2007 *Phys. Rev. Lett.* **99** 220403
[25] Eckardt A, Holthaus M, Lignier H, Zenesini A, Ciampini D, Morsch O and Arimondo E 2009 *Phys. Rev.* A **79** 013611
[26] Bergmann K, Theuer H and Shore B W 1998 *Rev. Mod. Phys.* **70** 1003
[27] Garanovich I L, Longhi S, Sukhorukov A A and Kivshar Y S 2012 *Phys. Rep.* **518** 1
[28] Longhi S 2009 *Laser Photon. Rev.* **3** 243
[29] Szameit A, Kartashov Y V, Heinrich M, Dreisow F, Keil R, Nolte S, Tünnermann A, Vysloukh V A, Lederer F and Torner L 2009 *Opt. Lett.* **34** 2700
[30] Szameit A, Kartashov Y V, Dreisow F, Heinrich M, Pertsch T, Nolte S, Tünnermann A, Vysloukh V A, Lederer F and Torner L 2009 *Phys. Rev. Lett.* **102** 153901